

Quorum Sensing Facilitates Interpopulation Signaling by *Vibrio fischeri* within the Light Organ of *Euprymna scolopes*

Taylor A. Yount^{+, [a]}, Andrew N. Murtha^{+, [a]}, Andrew G. Cecere,^[a] and Tim I. Miyashiro^{*[a]}

Abstract: Quorum sensing is an intercellular signaling mechanism that enables bacterial cells to coordinate population-level behaviors. How quorum sensing functions in natural habitats remains poorly understood. *Vibrio fischeri* is a bacterial symbiont of the Hawaiian bobtail squid *Euprymna scolopes* and depends on LuxI/LuxR quorum sensing to produce the symbiotic trait of bioluminescence. A previous study demonstrated that animals emit light when co-colonized by a Δlux mutant, which lacks several genes within the *lux* operon that are necessary for bioluminescence production, and a LuxI⁻ mutant, which cannot synthesize the

quorum signaling molecule *N*-3-oxohexanoyl-homoserine lactone. Here, we build upon that observation and show that populations of LuxI⁻ feature elevated promoter activity for the *lux* operon. We find that population structures comprising of Δlux and LuxI⁻ are attenuated within the squid, but a wild-type strain enables the LuxI⁻ strain type to be maintained *in vivo*. These experimental results support a model of interpopulation signaling, which provides basic insight into how quorum sensing functions within the natural habitats found within a host.

Keywords: quorum sensing · symbiosis · *Vibrio fischeri* · gene regulation · microbial ecology

1. Introduction

Quorum sensing describes the process by which bacterial cells use small signaling molecules, or autoinducers, to facilitate intercellular interactions that coordinate the expression of traits across a population.^[1,2] In many *Proteobacteria*, cytosolic LuxI family synthases produce acylated homoserine lactones (AHLs) that serve as autoinducers, which specifically bind to LuxR family transcription factors to regulate gene expression. AHLs freely diffuse across cell membranes, which can enable their accumulation within an environment as a bacterial population grows. Consequently, the expression of traits regulated by quorum sensing changes according to cell density. Traits that are regulated by quorum-sensing systems include bioluminescence, motility, biofilm formation, antimicrobial production, and, in pathogens, virulence factors.^[3,4,5,6]

The molecular underpinnings of quorum sensing have been determined primarily from studies based on growing bacterial samples in liquid cultures, which provides the reproducible conditions that are necessary for biochemical and genetic analysis of quorum-sensing pathways. In contrast, how quorum sensing functions in natural habitats is far less understood, largely due to the heterogeneous environments in which bacteria are commonly found.^[2] A particularly useful experimental platform to investigate quorum sensing within a natural habitat is the symbiosis established between the Hawaiian bobtail squid *Euprymna scolopes* and the bacterium *Vibrio fischeri*, which depends on quorum sensing to produce the symbiotic trait of bioluminescence.^[7] The squid possesses a light organ featuring several populations of *V. fischeri* that produce bioluminescence for the squid to conduct an anti-predatory behavior known as counter-illumination.^[8] The

symbiosis is initially established when a hatchling acquires environmental *V. fischeri* cells that successfully colonize the light organ.^[9] The nascent juvenile light organ consists of two lobes, with each lobe reproducibly featuring three separate epithelium-lined crypt spaces that serve as independent colonization sites for *V. fischeri*.^[10] The amenability of the light organ to light microscopy has facilitated the use of fluorescence-based tools to examine quorum sensing by *V. fischeri*.^[11,12]

Bioluminescence production by *V. fischeri* depends on the expression of the *lux* operon, which encodes light-emitting luciferase (LuxAB), a fatty acid reductase (LuxCDE), flavin mononucleotide reductase (LuxG), and autoinducer synthase LuxI (Figure 1A).^[3] LuxI, which is encoded by the first gene of the *lux* operon, synthesizes the autoinducer *N*-3-oxohexanoyl-homoserine lactone (3-oxo-C6 HSL) from S-adenosyl-methionine and hexanoyl-acyl carrier protein (ACP), with 5'-methyl-thioadenosine and apo-ACP as additional products.^[13] The gene encoding the transcription factor LuxR is divergently transcribed from the *lux* operon, and transcriptional regulation of *luxR* is regulated by additional quorum-sensing systems.^[14] Upon binding 3-oxo-C6 HSL, LuxR binds as a dimer to a 20-

[a] T. A. Yount,⁺ A. N. Murtha,⁺ A. G. Cecere, T. I. Miyashiro
Department of Biochemistry and Molecular Biology,
Microbiome Center, Huck Institutes of the Life Sciences,
The Pennsylvania State University
410 S. Frear Building, University Park, 16802, PA, USA
E-mail: tim14@psu.edu

[+] These authors contributed equally to this work.

Supporting information for this article is available on the WWW under <https://doi.org/10.1002/ijch.202200061>

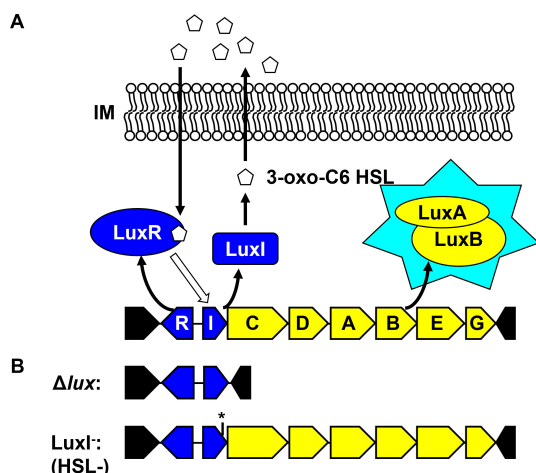


Figure 1. LuxI/LuxR quorum-sensing system of *V. fischeri*. **A.** Cartoon illustrating bioluminescence regulation by the LuxI/LuxR quorum-sensing system. The *lux* operon consists of seven genes (*luxICDABEG*), with *luxAB* encoding the heterodimeric luciferase enzyme that produces bioluminescence (cyan star). LuxI synthesizes autoinducer 3-oxo-C6 HSL (pentagon), which freely diffuses across the inner membrane (IM). LuxR is the transcription factor that binds to 3-oxo-C6 HSL and activates transcription of the *lux* operon. **B.** Mutants used in this study. The Δlux mutant harbors a deletion allele for *luxICDABEG* but retains the *luxI* gene. The LuxI⁻ mutant contains a 2-bp insertion within a BglIII site located near the 3'-end of the gene (asterisk) that causes a frameshift mutation.

bp *lux* box located upstream of the *lux* promoter (P_{lux}) and promotes transcriptional activation of the *lux* operon.^[15,16]

Bioluminescence production is necessary for *V. fischeri* to be maintained by *E. scolopes*. For instance, a mutant that lacks *luxCDABEG* (Δlux) (Figure 1B) is nonluminous and, although it can colonize the light organ, the mutant becomes attenuated by 48 h post-inoculation (p.i.).^[17] By 15 days p.i., the abundance of the Δlux mutant is below the limit of detection,^[18] which suggests that bioluminescence production contributes to fitness *in vivo*. In a separate study, squid colonized by a mutant unable to synthesize 3-oxo-C6 HSL (LuxI⁻) (Figure 1B) failed to emit bioluminescence and exhibited attenuated levels of *V. fischeri*,^[19] which indicates that quorum sensing is also important for establishment of the symbiosis. Consistent with this idea, a subsequent study found that treating LuxI⁻-colonized animals with 3-oxo-C6 HSL not only resulted in bioluminescence production but also restored wild-type levels of bacteria within the light organ,^[20] which demonstrates the ability of an exogenous source of autoinducer to induce bioluminescence production within the host.

The availability of the Δlux and LuxI⁻ mutants provided the opportunity to test whether the LuxI⁻ mutant could detect the autoinducer produced by the Δlux mutant within the light organ. Indeed, squid colonized by both strains exhibited bioluminescence,^[21] which highlighted that different strains can interact within the light organ via quorum sensing. Here, we expand upon this observation by showing that the

transcriptional activity of P_{lux} is elevated within LuxI⁻ populations in light organs that also feature the Δlux mutant. While the corresponding population structures are attenuated within the light organ, we find that replacement of the Δlux mutant with the parental wild-type strain results in the LuxI⁻ strain being maintained. Together, these experiments provide evidence that *V. fischeri* populations communicate across spatially segregated colonization sites via AHL signaling within the host, thereby increasing understanding of how quorum sensing functions in natural habitats.

2. Results

Previous work demonstrated that animals co-colonized with strains EVS102 (Δlux) and VCW2G7 (LuxI⁻) produced bioluminescence, even when the strain types were segregated in different crypts within the light organ.^[21] To investigate this two-strain model for autoinducer-mediated interactions, we initiated this study by attempting to replicate these results. Squid colonization assays were performed with derivatives of the Δlux and LuxI⁻ strains harboring plasmids that constitutively express YFP and CFP, respectively (Figure 2A). When squid were exposed to a single-strain inoculum containing either Δlux or LuxI⁻, none of the animals produced bioluminescence, *i.e.*, their bioluminescence levels were comparable to those squid in the apo group (Figure 2B). However, when the inoculum contained both strains at equal abundance, 86% (30/35) of the squid produced a level of bioluminescence greater than animals colonized by Δlux (Figure 2B). For each animal, we determined its colonization state, *i.e.*, the position of each strain type within its light organ, by fluorescence microscopy and scored the corresponding crypt spaces for YFP and CFP. With only one exception, all animals that were scored as bioluminescent had light organs featuring both strain types (Figure 2D). The one exception did not feature crypt spaces with fluorescence, which suggests the low bioluminescence reading was merely a false positive. Of the six animals that were not bioluminescent, only one had both strain types. With 97% (29/30) of animals co-colonized with Δlux and LuxI⁻ exhibiting bioluminescence, these data suggest that interactions between the two strain types promote bioluminescence production as previously reported.^[21]

In that report, another result associated with the animals co-colonized with Δlux and LuxI⁻ was that bioluminescence was detected even when the strains occupied different crypt spaces within the same light organ.^[21] To determine whether spatial segregation of strain types was a frequent outcome in animals co-colonized with the two strain types, we further examined the colonization states of animals in the experiment described above. Approximately 77% (23/30) of the co-colonized light organs featured crypt spaces with both strain types (Figure 2C), which suggests that conditions within our experiment permitted cells of each strain type to access and grow within the same crypt space in the majority of squid. Because the incidence of co-colonized crypts complicates the

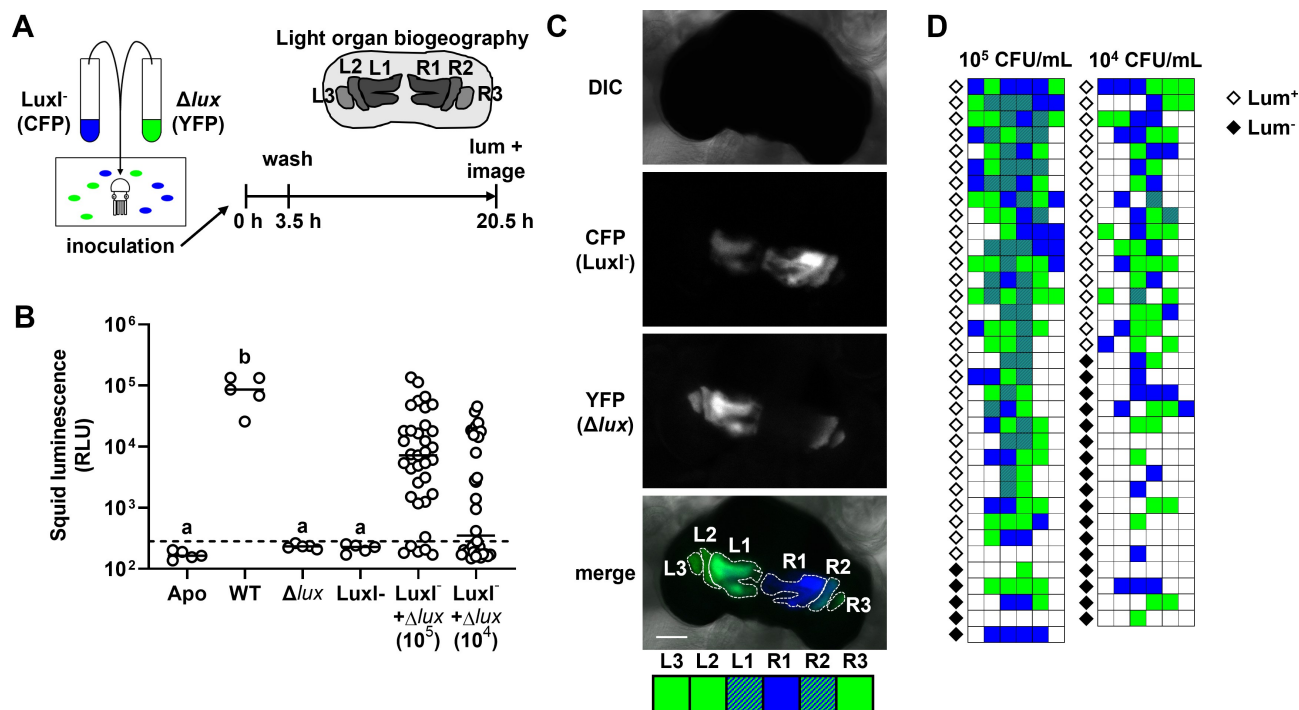


Figure 2. Squid co-colonized with Δlux and $LuxI^-$ emit bioluminescence. **A.** Experimental design. Squid are exposed as a group to the indicated inoculum for 3.5 h. At 20.5 hp.i., animals were assessed for bioluminescence and their light organs were examined for CFP and/or YFP fluorescence. Cartoon illustrates the biogeography of colonization sites within the light organ, with L and R corresponding to left and right crypt spaces. **B.** Bioluminescence levels of animals exposed to the indicated strains at 20.5 hp.i. Strains are ES114 (WT), EVS102 (Δlux), and VCW2G7 ($LuxI^-$), and harbor pYS112 (CFP) or pSCV38 (YFP). Apo=apo-symbiotic. Each point represents an individual squid, and bars represent group medians (N=5 for control groups, 34–35 for experimental groups). A one-way ANOVA detected statistically significant variation among means of log-transformed data for the four control groups ($F=340.4$, $p<0.0001$). A Tukey's *post-hoc* test was performed to determine statistical significance between group means of log-transformed data, with *p*-values adjusted for multiple comparisons (different letters indicating $p<0.0001$ and same letters indicating $p>0.05$). Dotted line indicates the bioluminescence cutoff based on 99th percentile of the Δlux group. RLU=relative light units. Inoculums for $LuxI^- + \Delta lux$ groups are 5×10^5 (10^5) and 5×10^4 (10^4) CFU/mL. **C.** Images of differential interference contrast (DIC), CFP fluorescence, YFP fluorescence, and merged image of a co-colonized light organ from B. Dotted lines and labels indicate the crypt spaces that contain a population of *V. fischeri* cells. Row of boxes indicates colonization state with colors indicating strain type(s) of corresponding crypt space (white=CFP⁻ YFP⁻; blue=CFP⁺ YFP⁻; green=CFP⁻ YFP⁺; blue/green stripes=CFP⁺ YFP⁺). Crypts are labeled as in A. Scale bar=100 μ M. **D.** Colonization profiles of $LuxI^-/\Delta lux$ groups shown in B. Each row indicates the colonization state of one individual animal as defined in C. Order is based on bioluminescence level (top row=highest bioluminescence). Diamonds indicate whether animal is scored as bioluminescent (Lum⁺, open) or non-bioluminescent (Lum⁻, closed).

assessment of interactions between spatially segregated populations within the light organ, we lowered the overall bacterial abundance from 5×10^5 CFU/mL to 5×10^4 CFU/mL within the inoculum mixed with Δlux and $LuxI^-$. While the frequency of bioluminescent squid decreased to 50% (17/34) (Figure 2B), only 18% (3/17) of them featured a crypt space containing both strain types (Figure 2D). Therefore, in subsequent experiments to investigate interpopulation interactions, we used the inoculum size of 10^4 CFU/mL to generate populations that were spatially segregated by strain type.

In bioluminescent animals that are co-colonized with Δlux and $LuxI^-$, only $LuxI^-$ encodes the luciferase enzyme. Therefore, we hypothesized that the *lux* genes were transcriptionally activated within the $LuxI^-$ populations. To assess transcriptional activity of the *lux* operon *in vivo*, we generated a $P_{lux}::cfp$ fusion by cloning 210 bp of the *lux* promoter region

upstream of the *cfp* gene within a reporter plasmid that is stably maintained by *V. fischeri*. To validate the $P_{lux}::cfp$ reporter, we grew the $LuxI^-$ strain harboring the plasmid in media containing different levels of 3-oxo-C6 HSL, which induces bioluminescence production by binding LuxR to activate it as a transcriptional regulator of the *lux* operon. Relative to the DMSO solvent control, 3-oxo-C6 HSL induced bioluminescence production by $LuxI^-$ in a dose-dependent manner (Figure 3A). Consistent with increased transcriptional activity of the *lux* operon, the level of CFP fluorescence also increased with autoinducer (Figure 3B), which suggests that the $P_{lux}::cfp$ construct can be used to assess P_{lux} activity.

We next evaluated whether the $P_{lux}::cfp$ reporter could be used to detect P_{lux} activity *in vivo*. A previous study demonstrated that treating animals exposed to the $LuxI^-$ mutant with 3-oxo-C6 HSL results in the production of bioluminescence,^[20]

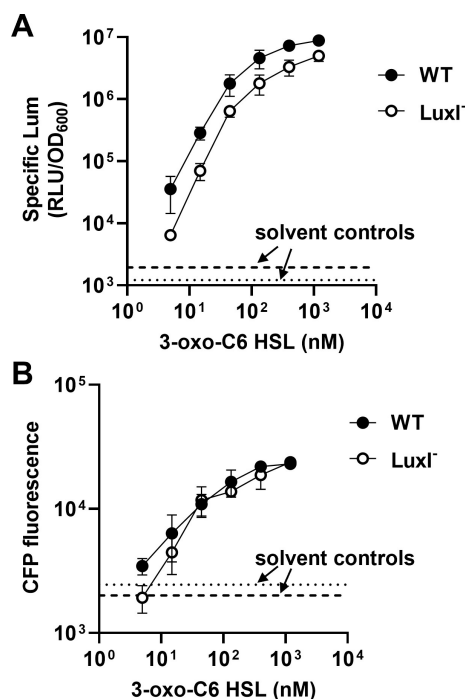


Figure 3. P_{lux} activity is elevated in *V. fischeri* cells emitting bioluminescence. **A.** Specific bioluminescence of ES114 (WT) and VCW2G7 (LuxI⁻) harboring the $P_{lux}::cfp$ reporter plasmid pTM424 in response to the indicated level of autoinducer (3-oxo-C6 HSL). Points and error bars represent the group means (N=3) and standard deviations, respectively. Dashed and dotted lines represent means of DMSO solvent control groups for WT and LuxI⁻, respectively. **B.** CFP fluorescence of samples shown in A. Points and error bars represent the group means (N=3) and standard deviations, respectively. Dashed and dotted lines represent means of DMSO solvent control groups for WT and LuxI⁻, respectively.

which suggests that the host-associated populations of LuxI⁻ can respond to an exogenous source of autoinducer. To assess P_{lux} transcriptional activity *in vivo*, we used a similar experimental setup by first exposing juvenile squid to an inoculum containing cells of LuxI⁻ harboring the $P_{lux}::cfp$ reporter and then treating them with 1 μ M 3-oxo-C6 HSL. Bacterial populations were identified by fluorescence of mCherry, which is constitutively expressed on the same plasmid containing the $P_{lux}::cfp$ reporter. Relative to the vehicle control, animals treated with 3-oxo-C6 HSL exhibited higher levels of bioluminescence (Figure 4A), which is consistent with the previous report.^[20] Furthermore, their light organs featured LuxI⁻ populations with higher levels of CFP fluorescence than the vehicle control (Figures 4B–D), which suggests the 3-oxo-C6 HSL treatment induced P_{lux} transcription. Together, these results suggest that transcription of the *lux* operon within host-associated populations increases in response to exogenous 3-oxo-C6 HSL and demonstrates that the $P_{lux}::cfp$ reporter can be used to assess P_{lux} activity *in vivo*.

To determine whether P_{lux} transcriptional activity is induced in LuxI⁻ populations in animals colonized by both

Δlux and LuxI⁻, we repeated the colonization assay described above using cells of the LuxI⁻ strain harboring the $P_{lux}::cfp$ reporter plasmid. In addition, the Δlux strain harbored a plasmid that expresses mCherry and YFP, with the latter fluorescent protein enabling us to identify Δlux populations. Co-colonization occurred at a frequency of 63% (22/35) (Figure 5A), with all co-colonized animals producing bioluminescence (Figure 5B). In 19/26 co-colonized animals, the light organ featured at least one crypt space containing only the LuxI⁻ strain type, which permitted quantification of the corresponding CFP fluorescence. In each case, the CFP fluorescence level was elevated relative to the LuxI⁻ control group (Figure 5C), which suggests that transcription of P_{lux} is activated within these populations.

Previous studies reported that CFU levels within animals colonized by LuxI⁻ decrease over time,^[19,20] which suggests that autoinducer production is necessary for *V. fischeri* to be maintained by the host. Because our data above suggest that Δlux can induce P_{lux} transcription in LuxI⁻ populations, we next tested whether animals co-colonized with Δlux and LuxI⁻ would maintain LuxI⁻. First, we used single-strain colonization assays to verify previous reports that the abundance of LuxI⁻ becomes attenuated by 72 h.p.i. (Figure 6A). Then, we examined the abundance of LuxI⁻ in animals exposed to an inoculum mixed evenly with Δlux and LuxI⁻. Relative to the WT control, animals exposed to the mixed-strain inoculum featured fewer CFU of each strain type (Figure 6B), which suggests that population structures composed of Δlux and LuxI⁻ cannot achieve normal colonization levels.

Previous work has shown that the Δlux mutant fails to be maintained, even in the presence of WT cells.^[18] Attenuation of the Δlux mutant in the mixed populations described above would remove the source of autoinducer, which in turn would subject nonluminescent LuxI⁻ cells to elimination by the host. However, these results also suggest that a strain competent for symbiosis, *i.e.*, able to synthesize autoinducer and produce bioluminescence, has the potential to serve as a stable source of autoinducer for an autoinducer-defective strain, thereby promoting its maintenance.

To determine whether autoinducer-defective populations are induced in light organs that also feature strain types that are competent for symbiosis, we examined the P_{lux} activity of LuxI⁻ populations within squid that were exposed to an inoculum containing LuxI⁻ and WT cells. We found 55% (18/33) of the squid were co-colonized (Figure 5A), with 16 of them featuring at least one crypt space colonized with only the LuxI⁻ strain type. Relative to the LuxI⁻ control group, each of the LuxI⁻ populations within squid co-colonized with WT and LuxI⁻ exhibited higher CFP fluorescence (Figure 5C), which suggests that P_{lux} was induced by the autoinducer produced by WT cells in a separate crypt space.

We then evaluated whether an autoinducer-defective strain is maintained in animals co-colonized with a symbiotic competent strain by exposing squid to an inoculum mixed with LuxI⁻ and WT cells. To distinguish between strain types, the LuxI⁻ and WT strains were labeled with CFP and YFP,

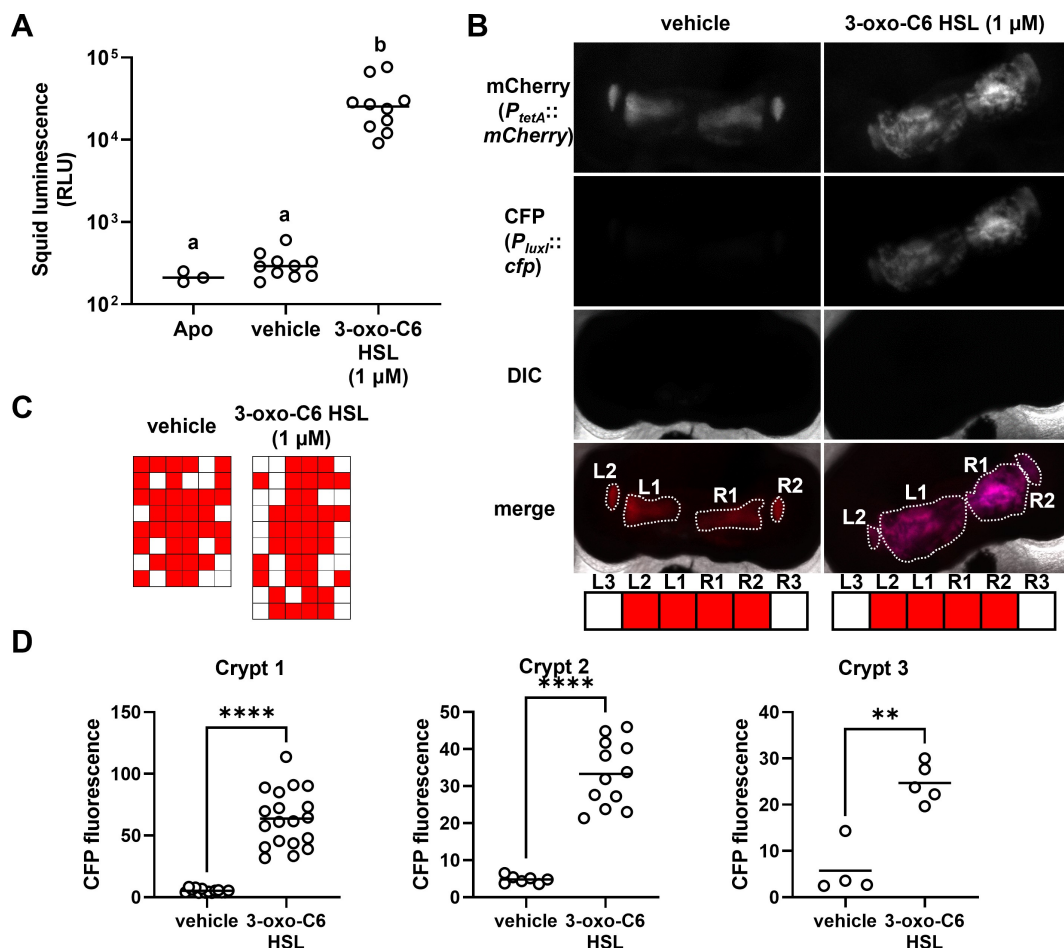


Figure 4. AI treatment induces P_{lux} activity *in vivo*. **A.** Bioluminescence of animals (24 h.p.i.) colonized by VCW2G7 ($LuxI^-$) harboring the $P_{lux}::cfp$ reporter plasmid pTM424 with DMSO solvent control (vehicle) or 3-oxo-C6 HSL treatment. Apo=apo-symbiotic. Each point represents an individual squid, and bars represent group means. A one-way ANOVA detected statistically significant variation among means of log-transformed data ($F=211.3$, $p<0.0001$). A Tukey's *post-hoc* test was performed to determine statistical significance between means of log-transformed data of groups, with p -values adjusted for multiple comparisons (different letters indicating $p<0.0001$ and same letters indicating $p>0.05$). **B.** Images of mCherry fluorescence (presence of bacteria), CFP fluorescence (P_{lux} activity), DIC and merge of representative light organs from \pm 3-oxo-C6 HSL groups in A. Dotted lines and labels indicate the crypt spaces that contain a population of *V. fischeri* cells. Boxes indicate the colonization state with a strain present (red) or absent (white) in each crypt space. **C.** Colonization states of groups in A, based on scheme in panel B. **D.** P_{lux} activity (CFP fluorescence) of crypt type for groups in A. Each point represents the average CFP fluorescence in an individual crypt space scored as positive for mCherry fluorescence. For each crypt type, an unpaired t-test with Welch's correction was performed to test for statistical significance between group medians (****= $p<0.0001$, **= $p<0.01$).

respectively. As a negative control, we included a group of animals exposed to an inoculum evenly mixed with $LuxI^-$ strains differentially labeled with CFP and YFP. Relative to the negative control, the abundance of the CFP-labeled $LuxI^-$ strain was higher in the presence of WT cells at 72 h.p.i. (Figure 6C), which suggests that an autoinducer-defective strain can be maintained by symbiotic strains *in vivo*.

3. Discussion

Quorum-sensing systems feature diffusible signaling molecules that enable bacterial cells to interact at a distance, but the

extent to which such interactions take place within a host remains poorly understood. In this study, we address this knowledge gap by capitalizing on the symbiosis that is established between *E. scolopes* and *V. fischeri*, which critically depends on quorum sensing for the symbiotic trait of bioluminescence production. In particular, our study was motivated by the observation that animals featuring spatially segregated populations of Δlux and $LuxI^-$ result in bioluminescence,^[21] which raised the possibility of interpopulation signaling *in vivo*. We found that inoculation conditions could control the frequency of co-colonized light organs featuring strain types localized to different crypt spaces (Figure 2), which further develops this two-strain system as an

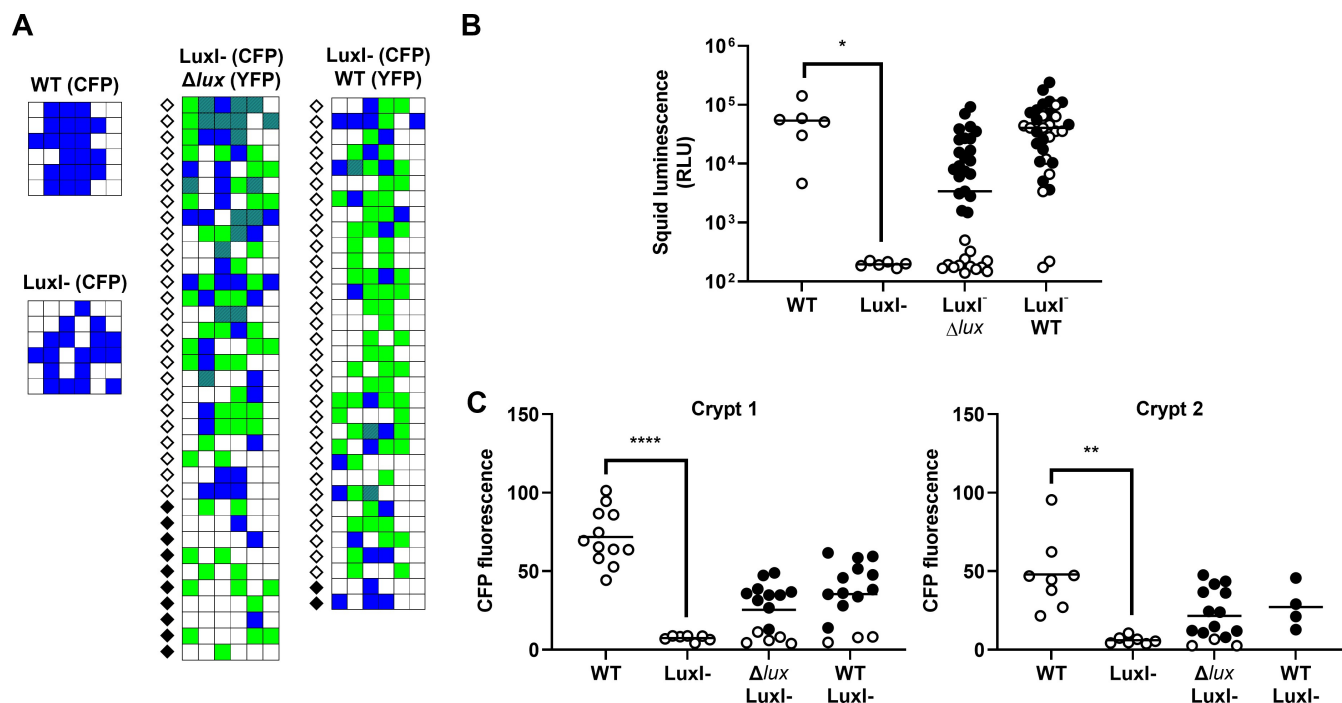


Figure 5. Induction of P_{lux} transcription by neighboring populations *in vivo*. **A.** Colonization states of animals exposed to ES114 (WT), VCW2G7 (LuxI⁻), or EVS102 (Δlux) harboring either the $P_{lux}::cfp$ reporter plasmid pTM424 (CFP) or pSCV38 (YFP). Each row represents an individual squid with white (mCherry), green = (mCherry⁺ YFP⁺), blue = (mCherry⁺ CFP⁺), blue/green stripes = (mCherry⁺ YFP⁺ CFP⁺). Diamonds represent animals that are bioluminescent (open) or dark (closed) relative to apo-symbiotic animals. **B.** Bioluminescence of squid in panel A at 20.5 h p.i. Each point represents an individual squid, and bars represent group medians. An unpaired, two-tailed *t*-test with Welch's correction detected statistically significant variation among means of log-normal data for control groups (**** = $p < 0.0001$). For groups involving mixed-strain inoculums, closed symbols indicate squid co-colonized with both strain types and open symbols indicate squid colonized by a single strain type. **C.** P_{lux} activity (CFP fluorescence) of crypts singly colonized with the strain harboring pTM424 for squid shown in A. Each point represents the average CFP fluorescence pixel value of a region of interest that exhibits mCherry fluorescence but no YFP fluorescence, and bars represent group medians. Closed symbols indicate the crypt was within a co-colonized animal, and open symbols represent crypts from animals colonized with only one strain type. *Left*, crypt 1; *right*, crypt 2. Unpaired *t*-tests with Welch's correction were used to determine whether means are statistically significantly different (**** = $p < 0.0001$, ** = $p = 0.0013$).

experimental platform to investigate interpopulation signaling *in vivo*. We found that autoinducer can induce P_{lux} activity within each crypt space (Figure 4), which highlights the potential for a population within any crypt space to be induced by an exogenous source of autoinducer. P_{lux} activity is elevated in LuxI⁻ populations that are spatially segregated from other populations within co-colonized animals (Figure 5). Finally, we provide evidence that strains that are defective for autoinducer synthesis can be maintained in animals that are also colonized with symbiotic strains (Figure 6), which provides a potential function for interpopulation signaling after the initial assembly of symbionts.

From these data, we propose a model for interpopulation signaling within the squid light organ (Figure 7). Upon accessing a crypt space, founder *V. fischeri* cell(s) will grow on host-derived sources of nutrients and energy to fill the corresponding site. The increase in cell density promotes bioluminescence production by means of higher rate of autoinducer synthesis, which activates transcription of the *lux* operon. However, through diffusion, autoinducer can enter

neighboring crypt spaces, thereby adding to the local concentration of the signaling molecule. Consequently, a population neighboring another population that synthesizes large amounts of autoinducer may boost bioluminescence production.

Because organogenesis results in the nascent light organ featuring six distinct colonization sites,^[10] the symbiosis between *E. scolopes* and *V. fischeri* offers a reproducible experimental platform to investigate how bacterial biogeography impacts quorum sensing in a natural habitat, which represents a major challenge in many systems.^[2] Here, we have observed evidence of interpopulation signaling, *i.e.*, autoinducer-producing populations promoting bioluminescence production or P_{lux} activity, in various arrangements: i) populations in distal crypts (crypt types 2 and 3) induced by a population in crypt 1; ii) a population in crypt 1 induced by populations in distal crypts; and iii) populations within one lobe of the light organ induced by populations in the other lobe. Within the juvenile light organ, the distance between crypt spaces can range from several microns for adjacent crypt spaces (L1-L2 or R1-R2) to hundreds of microns for other

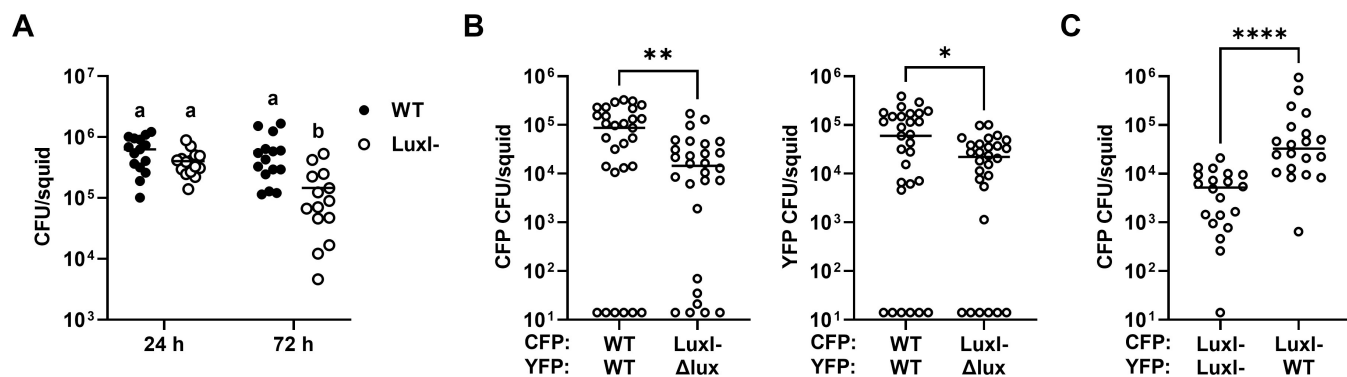


Figure 6. Maintenance of LuxI⁻ *in vivo* depends on the presence of a symbiotic strain. **A.** Abundance of ES114 (WT, closed symbols) or VCW2G7 (LuxI⁻, open symbols) at 24 h and 72 h p.i from single-strain colonization assays. Each point represents an individual squid exposed to the indicated strain, and bars represent group means. A two-way ANOVA analysis of log-transformed data revealed statistical significance among group means due to time ($F_{1,55}=14.50$, $p=0.0004$), genotype ($F_{1,55}=19.08$, $p<0.0001$), and their interaction ($F_{1,55}=8.450$, $p=0.0050$). A Sidak's post-hoc test was performed to determine statistical significance between means of log-transformed data of groups, with p -values adjusted for multiple comparisons (different letters indicating $p<0.0001$ and same letters indicating $p>0.05$). **B.** Abundance of strains labeled with CFP (left) and YFP (right) in squid at 72 h.p.i. Each point represents an individual squid, and bars represent group medians. Squid were exposed to inoculum mixed with ES114 (WT), VCW2G7 (LuxI⁻), or EVS102 (Δlux) harboring either pYS112 (CFP) or pSCV38 (YFP). For each data set, an un-paired Mann-Whitney test was used to test for statistical significance between group medians (**= $p=0.0096$, *= $p=0.0485$). **C.** Abundance of VCW2G7 (LuxI⁻) harboring pYS112 (CFP) in squid at 72 h.p.i. Each point represents an individual squid, and bars represent group medians. Squid were exposed to inoculum mixed with the CFP-labeled LuxI⁻ strain and either VCW2G7 (LuxI⁻) or ES114 (WT) harboring plasmid pSCV38 (YFP). A Mann-Whitney test was used to test for statistical significance between group medians (****= $p<0.0001$).

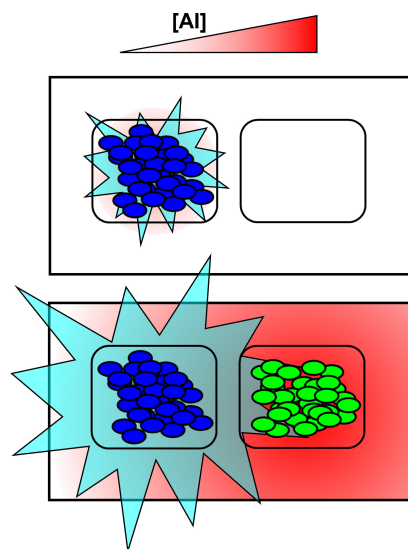


Figure 7. Model of interpopulation quorum signaling *in vivo*. *Top*, a single population of *V. fischeri* cells (blue) within a light organ crypt space produces bioluminescence (cyan) according to the AI (red) generated by that population. *Bottom*, the same population near a population comprising of a strain that synthesizes high levels of AI (green) responds with higher bioluminescence production.

pairings (e.g., L1-R2, L3-R3, etc.). Previous analysis of AHL diffusion properties suggests that the distances over which AHLs can travel and induce quorum sensing, i.e., ‘calling distances’, are typically well under 100 μm .^[22] Consequently, the unusually large calling distances that can occur within the

light organ suggest that its physicochemical properties promote interpopulation signaling. In support of this idea, previous work with radiolabeled autoinducer demonstrated that autoinducer can freely diffuse into the central core tissue of light organs where *V. fischeri* are located within adult squid.^[23] We anticipate approaches based on single-molecule tracking to be particularly useful in resolving the diffusion dynamics of AHLs within the squid light organ.

In other bacteria, quorum sensing promotes cooperative behaviors within a population by inducing the expression of certain enzymes that are secreted into the extracellular environment and provide a benefit to any cell within that environment. Such enzymes are referred to as ‘public goods’, and because their production represents a cost, strains that do not produce public goods have the potential to exploit the cooperative behavior as ‘cheaters’ with increased fitness relative to cooperative cells.^[2] At first glance, the Δlux mutant appears to have the hallmarks of a cheater: the mutant does not contribute to bioluminescence production within a population and grows faster than the wild-type strain under quorum-sensing conditions.^[17] However, independent studies with this mutant have demonstrated that the abundance of Δlux decreases in animals co-colonized with the wild-type strain,^[12,17,18] which suggests that the host plays a role in lowering the fitness of the mutant such that it cannot cheat *in vivo*. The population collapse observed for animals co-colonized with Δlux and LuxI⁻ (Figure 5B) provides additional evidence of this hypothesis and furthermore suggests that a stable symbiosis depends on each strain producing bioluminescence. These findings also emphasize the significance

of bioluminescence production in the maintenance of the symbiosis. Future studies will first examine the physiology of nonluminous strains *in vivo* to gain insight into how the mutant is eliminated from the squid light organ, which in turn, will provide a foundation for elucidating the mechanisms by which the host selects for bioluminescent strains.

Because the light organ of *E. scolopes* features multiple strains of *V. fischeri* in nature,^[24–26] the symbiosis has become a powerful experimental system to examine how strain diversity initially forms and is maintained. After crypt spaces are initially colonized, the corresponding bacterial populations experience daily expulsion events,^[27,28] with the majority of cells being released into the marine environment. The few cells remaining within each crypt space grow and repopulate the site, and a recent study provided evidence that these subsequent rounds of population growth promoted further diversification.^[29] The model of interpopulation signaling presented here provides a potential source of selective pressure because cells must balance producing sufficient bioluminescence for the host with its energetic cost. Exposure to a high level of autoinducer *in vivo* may select over time for mutants with decreased luciferase activity that compensates for the enhanced induction of the *lux* operon. Alternatively, a dim strain that would otherwise be eliminated may be sustained by exogenous autoinducer and evolve higher LuxI activity that further enhances bioluminescence production *in vivo*. Consistent with this idea of local adaptation *in vivo*, strains isolated directly from the light organ of wild-caught squid produce different levels of bioluminescence.^[24,25,30] Future studies will investigate the extent to which *V. fischeri* quorum sensing adapts *in vivo*, thereby increasing understanding of how the biogeography of symbionts within a host affects their evolution.

4. Materials and Methods

Media and growth conditions. *V. fischeri* strains (Table 1) were routinely grown aerobically at 28 °C in LBS medium (1% [wt/vol] tryptone, 0.5% [wt/vol] yeast extract, 2% [wt/vol] NaCl, 50 mM Tris-HCl [pH 7.5]) or SWTO medium (0.5% [wt/vol] tryptone, 0.3% [wt/vol] yeast extract, 0.3% [vol/vol] glycerol, 0.88% [wt/vol] NaCl, and 70% [vol/vol] Instant Ocean

seawater). For strains harboring a plasmid (Table 1), the medium was supplemented with chloramphenicol at 2.5 µg/mL. Liquid cultures were incubated on a platform shaker set at 200 rpm.

pTM424 construction. To construct pTM424, which contains the $P_{lux}::cfp$ transcriptional reporter, primers luxI-prom-XmaI-u1 (GAGGTACCAGCGTGCCAACTTTTTACCCGTA) and luxI-prom-XbaI-l1 (TTCTAGATACAGCCATGCAACCTCTCT) were used to amplify the P_{lux} region from ES114 genomic DNA by PCR with PFU Ultra according to instructions from the manufacturer. The resulting amplicon was cloned into pCR-blunt, validated by Sanger sequencing, and sub-cloned into pSCV37 via XbaI/XmaI.

Squid colonization assay. For each strain, a starter culture in LBS medium with chloramphenicol was incubated overnight. A 30-µL volume was diluted into 3 mL fresh LBS medium with antibiotic. At OD₆₀₀ = 1.0, cultures were serially diluted into 50 mL filter-sterilized seawater (FSSW). To initiate the assay, the cell suspension was poured into a plastic tumbler containing 50 mL FSSW and newly hatched juvenile squid that were generated by a mariculture facility as described elsewhere.^[31] Inoculum levels were determined by serially diluting the inoculum and plating cell suspensions onto solid LBS medium. In this study, inoculums were approximately 50,000 total CFU/mL, except for the groups containing 500,000 CFU/mL (10⁵) shown in Figure 2. After 3.5 h, each squid was washed by serial transferring them into 100 mL FSSW for five minutes twice and then transferring them individually into a vial containing 4 mL FSSW. Where indicated, FSSW contained 1 µM 3-oxo-C6 HSL, with the final concentration of DMSO solvent not exceeding 0.1% (v/v), which is lower than previously used concentrations.^[20] Squid were maintained at room temperature with a 12-h dark/12-h light lighting schedule. After 20.5 h, each animal was transferred to a new vial containing 4 mL FSSW, and its bioluminescence was measured using a GloMax 20/20 Luminometer (Promega, USA).

Abundance of *V. fischeri* within a squid was determined by first anesthetizing the animal and then cryopreserving the animal at –80 °C for at least 24 h. Animals were thawed on ice and then homogenized with a pestle in 0.7 mL 70% Instant Ocean seawater. The resulting homogenate was serially diluted, plated onto LBS, and incubated at 28 °C. After 24 h, the resulting CFU were enumerated and scored for YFP and CFP fluorescence using an Olympus SX16 fluorescence dissecting microscope (Olympus Corp., Tokyo, Japan) equipped with YFP and CFP filter sets.

Imaging of the light organ by fluorescence microscopy was performed by first anesthetizing the animals on ice. After five minutes, animals were exposed to 1 mL cold 4% paraformaldehyde/marine phosphate buffered saline (mPBS) and maintained at 4 °C. After 24 h, the fixed animals were washed three times in 1 mL mPBS. Squid were dissected to reveal the light organ by removing the mantle and digestive tissue. A Zeiss 780 confocal microscope (Carl Zeiss AG, Germany) was used to obtain 8-bit images of CFP

Table 1. Strains and plasmids used in this study.

Strain name	Genotype	Reference
ES114	Wild-type <i>V. fischeri</i>	[33]
VCW2G7	ES114 <i>luxI</i> (2-bp frameshift)	[19]
EVS102	ES114 $\Delta luxCDABEG$	[17]
Plasmid name	Genotype	Reference
pSCV37	$P_{tetA}::cfp$ $P_{tetA}::mCherry$	[12]
pSCV38	$P_{tetA}::yfp$ $P_{tetA}::mCherry$	[25]
pTM424	$P_{lux}::cfp$ $P_{tetA}::mCherry$	This work
pVSV105	Vector control	[11]

fluorescence, YFP fluorescence, mCherry fluorescence, and DIC, with pinholes set to maximum opening to mimic epifluorescence settings.

Collection, care, and research of all laboratory animals was completed under the program's Institutional Animal Care and Use Committee (IACUC). IACUC protocol # PRO-TO202101789.

Bioluminescence assay. A starter culture in LBS medium with chloramphenicol was inoculated with an isolated colony of the indicated strain and incubated overnight. The culture was normalized to $OD_{600}=1.0$ and diluted 1/100 into SWTO medium supplemented with antibiotic and the indicated amount of 3-oxo-C6 HSL in dimethyl sulfoxide as a solvent. In all experiments, DMSO did not exceed 0.1% (v/v). At $OD_{600}=1.0$, a 0.1-mL sample was transferred to a plastic cuvette and assessed for bioluminescence levels in a GloMax 20/20 Luminometer. To determine optical density, a 0.9-mL volume of medium was added to the cuvette, and the turbidity of the diluted sample was measured using a Biophotometer (Eppendorf, Germany). To calculate specific luminescence, each bioluminescence measurement was divided by the corresponding turbidity measurement.

P_{lux} in vitro expression assay. Culture samples were prepared for fluorescence and turbidity measurements as previously described.^[32] The CFP fluorescence (458 ex/477 em) and OD_{600} of each well were measured using a Tecan M1000Pro fluorescence plate reader (Tecan, Salzburg, Austria). A culture of non-fluorescent cells (pVSV105/ES114) was used to generate a linear standard curve to calculate the background fluorescence as a function of OD_{600} (0.1–1.0, 0.1 increments). CFP fluorescence was calculated by subtracting the calculated background and then normalizing by the corresponding OD_{600} .

P_{lux} in vivo expression assay. To quantify the CFP fluorescence for populations of *V. fischeri* harboring the $P_{lux}::cfp$ reporter plasmid pTM424, a multi-step image analysis approach was performed using ImageJ, v. 1.52a (NIH, USA). First, each population was located by subjecting the corresponding mCherry image to thresholding (default setting with minimum pixel value=23). Crypt spaces that overlap within the image were segmented by manually drawing lines using the Paintbrush tool (Brush width=2; Color=White). The resulting binary image was then subjected to the Analyze Particle function with 50-infinity size range and manually curating the results. Each population was scored for YFP fluorescence (Δlux), and those populations scored as negative for YFP fluorescence were further analyzed for CFP fluorescence by measuring the average pixel value.

Statistical analysis. All statistical analyses were performed using GraphPad Prism version 9.4.1 (GraphPad Software, LLC).

Acknowledgements

This work was supported by the National Institute of General Medical Sciences R01 GM129133 (to T. I. M.) and the Beckman Scholars Program (to T. A. Y.). We also thank members of the Miyashiro lab and three anonymous reviewers for constructive feedback on earlier manuscript drafts.

Data Availability Statement

The data that support the findings of this study are available in the supplementary material of this article.

References

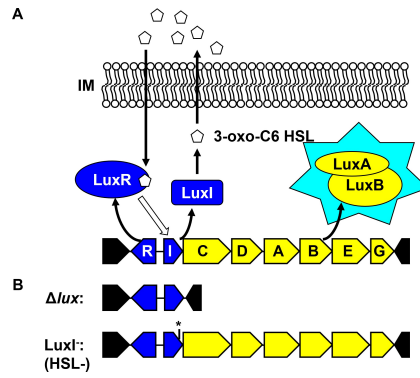
- [1] A. A. Bridges, J. A. Prentice, N. S. Wingreen, B. L. Bassler, *Annu. Rev. Microbiol.* **2022**.
- [2] M. Whiteley, S. P. Diggle, E. P. Greenberg, *Nature* **2017**, *551*, 313–320.
- [3] T. Miyashiro, E. G. Ruby, *Mol. Microbiol.* **2012**, *84*, 795–806.
- [4] A. M. Tsou, E. M. Frey, A. Hsiao, Z. Liu, J. Zhu, *Commun Integr Biol* **2008**, *1*, 42–44.
- [5] A. A. Bridges, B. L. Bassler, *PLoS Biol.* **2019**, *17*, e3000429.
- [6] M. Schuster, E. P. Greenberg, *Int. J. Med. Microbiol.* **2006**, *296*, 73–81.
- [7] S. C. Verma, T. Miyashiro, *Int. J. Mol. Sci.* **2013**, *14*, 16386–16401.
- [8] B. W. Jones, M. K. Nishiguchi, *Mar. Biol.* **2004**, *144*, 1151–1155.
- [9] K. H. Lee, E. G. Ruby, *J. Bacteriol.* **1994**, *176*, 1985–1991.
- [10] M. K. Montgomery, M. McFall-Ngai, *Biol. Bull.* **1993**, *184*, 296–308.
- [11] A. K. Dunn, D. S. Millikan, D. M. Adin, J. L. Bose, E. V. Stabb, *Appl. Environ. Microbiol.* **2006**, *72*, 802–810.
- [12] S. C. Verma, T. Miyashiro, *Appl. Environ. Microbiol.* **2016**, *82*, 5990–5996.
- [13] A. L. Schaefer, B. L. Hanzelka, A. Eberhard, E. P. Greenberg, *J. Bacteriol.* **1996**, *178*, 2897–2901.
- [14] T. Miyashiro, M. S. Wollenberg, X. Cao, D. Oehlert, E. G. Ruby, *Mol. Microbiol.* **2010**, *77*, 1556–1567.
- [15] A. M. Stevens, K. M. Dolan, E. P. Greenberg, *Proc. Natl. Acad. Sci. USA* **1994**, *91*, 12619–12623.
- [16] K. A. Eglund, E. P. Greenberg, *Mol. Microbiol.* **1999**, *31*, 1197–1204.
- [17] J. L. Bose, C. S. Rosenberg, E. V. Stabb, *Arch. Microbiol.* **2008**, *190*, 169–183.
- [18] E. J. Koch, T. Miyashiro, M. J. McFall-Ngai, E. G. Ruby, *Mol. Ecol.* **2014**, *23*, 1624–1634.
- [19] C. Lupp, M. Urbanowski, E. P. Greenberg, E. G. Ruby, *Mol. Microbiol.* **2003**, *50*, 319–331.
- [20] S. V. Studer, J. A. Schwartzman, J. S. Ho, G. D. Geske, H. E. Blackwell, E. G. Ruby, *Environ. Microbiol.* **2014**, *16*, 2623–2634.
- [21] A. N. Septer, E. V. Stabb, *PLoS One* **2012**, *7*, e49590.
- [22] A. W. Decho, R. L. Frey, J. L. Ferry, *Chem. Rev.* **2011**, *111*, 86–99.
- [23] K. J. Boettcher, E. G. Ruby, *J. Bacteriol.* **1995**, *177*, 1053–1058.
- [24] M. S. Wollenberg, E. G. Ruby, *Appl. Environ. Microbiol.* **2009**, *75*, 193–202.

- [25] Y. Sun, E. D. LaSota, A. G. Cecere, K. B. LaPenna, J. Larios-Valencia, M. S. Wollenberg, T. Miyashiro, *Appl. Environ. Microbiol.* **2016**, *82*, 3082–3091.
- [26] L. Speare, A. G. Cecere, K. R. Guckes, S. Smith, M. S. Wollenberg, M. J. Mandel, T. Miyashiro, A. N. Septer, *Proc. Natl. Acad. Sci. USA* **2018**, *115*, E8528–E8537.
- [27] K. J. Boettcher, E. G. Ruby, M. J. McFall-Ngai, *J. Comp. Physiol.* **1996**, *179*, 65–73.
- [28] L. K. Sycuro, E. G. Ruby, M. McFall-Ngai, *J. Morphol.* **2006**, *267*, 555–568.
- [29] C. Bongrand, E. Koch, D. Mende, A. Romano, S. Lawhorn, M. McFall-Ngai, E. F. DeLong, E. G. Ruby, *Front. Microbiol.* **2022**, *13*, 854355.
- [30] J. L. Bose, M. S. Wollenberg, D. M. Colton, M. J. Mandel, A. N. Septer, A. K. Dunn, E. V. Stabb, *Appl. Environ. Microbiol.* **2011**, *77*, 2445–2457.
- [31] A. G. Cecere, T. I. Miyashiro, *Lab. Anim. Res.* **2022**, *38*, 25.
- [32] N. P. Wasilko, J. Larios-Valencia, C. H. Steingard, B. M. Nunez, S. C. Verma, T. Miyashiro, *Mol. Microbiol.* **2019**, *111*, 621–636.
- [33] M. J. Mandel, E. V. Stabb, E. G. Ruby, *BMC Genomics* **2008**, *9*, 138.

Manuscript received: August 25, 2021

Revised manuscript received: September 30, 2022

Version of record online: ■■, ■■



T. A. Yount, A. N. Murtha, A. G. Cecere, T. I. Miyashiro*

1 – 11

Quorum Sensing Facilitates Interpopulation Signaling by *Vibrio fischeri* within the Light Organ of *Euprymna scolopes*

